Ocean Sci. Discuss., 10, 1505–1524, 2013
www.ocean-sci-discuss.net/10/1505/2013/
doi:10.5194/osd-10-1505-2013

Ocean Science
Discussions
Open Access

Geostrophic currents and kinetic energies in the Black Sea estimated from merged drifter and satellite altimetry data

M. Menna and P. -M. Poulain

Istituto Nazionale di Oceanografia e Geofisica Sperimentale – OGS, Trieste, Italy

Received: 30 July 2013 – Accepted: 21 August 2013 – Published: 4 September 2013

Correspondence to: M. Menna (mmenna@ogs.trieste.it)

Published by Copernicus Publications on behalf of the European Geosciences Union.

Geostrophic currents and kinetic energies in the Black Sea

M. Menna and P. -M. Poulain

Abstract

Drifter measurements and satellite altimetry data are merged to reconstruct the surface geostrophic circulation of the Black Sea in the period 1999–2009. This combined dataset is used to estimate pseudo-Eulerian velocity statistics for different time periods. Seasonal and interannual variability of currents and kinetic energy fields are described with particular attention to the mesoscale and sub-basin coastal eddies. The mean currents are generally stronger in winter and enhanced speeds are observed in the period 2002–2006. The most intense activity of sub-basin Batumi Eddy occurs in summer with greater speeds and dimensions in 2006 and 2008. The sub-basin Sevastopol Eddy is generated in spring from a meander of the Rim Current. Mesoscale eddies located along the Anatolia, Caucasus and Crimea coasts are permanent, quasi-permanent or intermittent features and can interact and merge with each other, showing higher values of kinetic energy.

1 Introduction

The geostrophic velocities derived from drifter and satellite altimetry are combined to describe the Black Sea (BS) surface circulation, and its seasonal and interannual variabilities. The combination of these two independent datasets has already been used to produce quantitative descriptions of the circulation in several areas of the ocean, such as the California Current System (Centurioni et al., 2008), the South China Sea (Centurioni et al., 2009), the Kuroshio Extension (Niiler et al., 2003), the North Pacific (Uchida and Imawaki, 2003) and the Mediterranean Sea (Menna et al., 2012; Poulain et al., 2012). The main advantages of this method are: (1) the removal of biases that arise from the irregular sampling of drifters, (2) the enhancement of the accuracy of velocity estimates in the coastal areas and (3) a more accurate representation of the mean circulation with respect to the computation performed from each dataset alone. The combined method, applied to concurrent satellite and drifter observations, gives an estimation of the Mean Dynamic Topography (MDT) of the BS in terms of absolute geostrophic velocity field, over the period 1999–2009.

A first attempt to estimate a MDT for the BS based on in-situ and satellite data was made by Kubryakov and Stanichny (2011), applying the synthetic method described by Rio et al. (2004, 2007). This synthetic MDT (SMDT) was computed over the period 1993–1999 using measurements of drifter velocities, hydrological data and along-track sea level anomalies (SLA). The SMDT defines the basin scale cyclonic along-slope Rim Current (RC), two separate cyclonic cells in the western and eastern part of the BS and some mesoscale features with anticyclonic vorticity near the periphery of the basin.

The goal of this paper is to produce a new MDT of the BS, so as to describe quantitatively the pathways and the spatio-temporal variability of the surface circulation in different regions of the basin. The paper is organized as follows: information on drifter, remotely sensed altimetry data and wind products is given in Sect. 2, followed by a description of the methods used to compute the surface geostrophic field. Pseudo-Eulerian statistics, seasonal and interannual characteristics and eddy variability are presented and discussed in Sect. 3. The main conclusions are summarized in Sect. 4.

2 Data and methods

The Lagrangian data used in this study come from 89 satellite-tracked drifters (SVP, CODE and CMOD designs) deployed in the BS between 1999 and 2009. They measure the near-surface currents in the first 15 m of the water column with various accuracies and errors induced by wind and waves (Poulain et al., 2009). The drifter position time series were edited to remove spike and outliers and linearly interpolated at 2 h intervals using the kriging technique (Poulain et al., 2004). The interpolated positions were low-pass filtered (Hamming filter with cut-off period at 36 h) to remove high frequency current components and sub-sampled at 6 h intervals. Velocity components were then estimated from centered finite differences of the 6 h positions and finally archived in a

Discussion Paper | Discussion Paper | Discussion Paper | Discussion Paper |

OSD

10, 1505–1524, 2013

Geostrophic currents and kinetic energies in the Black Sea

M. Menna and P. -M. Poulain

Title Page
Abstract Introduction
Conclusions References
Tables Figures
◀◀ ▶▶
◀ ▶
Back Close
Full Screen / Esc
Printer-friendly Version
Interactive Discussion

database (http://doga.ogs.trieste.it/sire/medsvp/). The pseudo-Eulerian velocity statistics directly computed with the drifter data are defined as 'biased' because the drifter data are usually non-uniformly sampled in space and time (Centurioni et al., 2008; Menna et al., 2012; Poulain et al., 2012).

Cross-Calibrated, Multi-Platform (CCMP) ocean surface wind velocities (Atlas et al., 2009) were filtered and interpolated at the drifter locations and times, then used with the drifter velocities in a linear regression model in order to estimate the currents directly (slippage) and indirectly (Ekman currents) induced by the winds ($U_{\text{wind-driven}}$). In this work we have used the results of the regression model applied in the Mediterranean Sea by Poulain et al. (2012):

$$U_{\text{wind-driven}} + \text{error} = \beta^{i\theta} W + \text{error}, \tag{1}$$

where β is a real constant and θ is the angle (positive anticlockwise) which represent, respectively, the estimations of intensity and the direction of drifter wind-driven currents with respect to the wind speed; W is the wind velocity interpolated at the drifter locations and times. The model was applied to the different drifter designs separately. The coefficients β and θ are drawn from the results obtained in the Mediterranean Sea from Poulain et al. (2012).

Finally, the wind-driven currents were subtracted from the drifter velocities to obtain the geostrophic components U_{DG} ($U_{\text{DG}} = U - U_{\text{wind-driven}}$). Details of this method are explained in Menna et al. (2012) and Poulain et al. (2012).

The altimetry data used in this work are gridded (1/8° Mercator projection grid) Ssalto/Duacs daily, multi-mission, delayed time products from AVISO (SSALTO/DUACS users handbook 2013). SLA data are defined with respect to a 7 yr mean (1993–1999). Because of the intermittent temporal distribution and the scarcity of the drifter data (not shown), daily altimetry products were preferred to weekly products in order to have a larger number of drifter-satellite concurrent observations.

Drifter geostrophic velocities and satellite altimetry data were averaged in non-overlapping geographical bins of 0.25° × 0.25° × 1 day and combined in the following

OSD
10, 1505–1524, 2013

regression model, according to the method described in Poulain et al. (2012):

$$U_{DG} = AU_{SLA} + B + \text{error}, \quad (2)$$

where U_{SLA} is the bin-averaged anomalies of surface geostrophic velocities, concurrent with the bin-averaged drifter geostrophic velocities U_{DG}; the slope A is the local adjustment of amplitude of U_{SLA}; B is the offset between U_{SLA} and U_{DG} and represents the MDT expressed in terms of geostrophic velocities in the period 1999–2009. Following Poulain et al. (2012), the slope A was subsequently low-pass filtered in $0.75^\circ \times 0.75^\circ$ overlapping bins to remove insignificant noise. The vector complex correlation (Kundu, 1976) between U_{DG} and U_{SLA} (Fig. 1a) is generally larger than 0.6 in the BS region, supporting the validity of the approach described by Eq. (2); correlation is low west of the Crimean Peninsula and off southern Bulgaria. The magnitude of the low pass filtered $|A|$ and of B are shown in Fig. 1b and c, respectively. The magnitude of $|A|$ varies mostly between 0.5 and 1.5; it exceeds 1.5 in the center of the BS basin and off the northern coast of Bulgaria. Deviation of A from unity is mainly due to the oversmoothing of the satellite altimeter data and to the existence of residual wind-driven components, non-linear boundary currents and ageostrophic acceleration in the drifter velocities (Niiler et al., 2003; Poulain et al., 2012). The offset B is as large as $30\,\text{cm s}^{-1}$ in the fast RC, in particular along the Anatolian and Crimean coasts, and smaller than $5\,\text{cm s}^{-1}$ in the interior of the basin. The relationship between drifter velocities and satellite SLA (A and B), derived from 11 yr of concurrent data (1999–2009), can be used to estimate the mean unbiased absolute geostrophic currents $\langle U_G \rangle_u$ for any time period in which U_{SLA} is available, independently from the availability of drifter data:

$$\langle U_G \rangle_u = A \langle U_{SLA} \rangle_u + B, \quad (3)$$

where U_G are the surface geostrophic currents and $\langle \rangle_u$ indicates the "unbiased" temporal averages in each spatial bin. The pseudo-Eulerian statistics computed with the combined geostrophic currents are defined as 'unbiased' because they are less affected by the non-uniform drifter sampling (Menna et al., 2012; Poulain et al., 2012).

OSD
10, 1505–1524, 2013

M. Menna and P. -M. Poulain

The interannual variability of the geostrophic circulation was assessed using the annual maps of kinetic energy of the mean flow per unit mass (MKE) and of mean kinetic energy of the residuals per unit of mass (eddy kinetic energy – EKE). The MKE is defined as:

$$\mathrm{MKE} = \frac{1}{2}\left(\langle U_\mathrm{G}\rangle_u^2 + \langle V_\mathrm{G}\rangle_u^2\right) \quad (4)$$

The residuals of geostrophic velocity field were evaluated removing the mean unbiased velocity $\langle U_\mathrm{G}\rangle_\mathrm{u}$ from each daily value of U_G ($U'_\mathrm{G} = U_\mathrm{G} - \langle U_\mathrm{G}\rangle_\mathrm{u}$) and the EKE is defined as:

$$\mathrm{EKE} = \frac{1}{2}\left(\left\langle U'^2_\mathrm{G}\right\rangle_\mathrm{u} + \left\langle V'^2_\mathrm{G}\right\rangle_\mathrm{u}\right) \quad (5)$$

The seasonal and interannual variability of mesoscale and sub-basin scale eddies in the BS was investigated in terms of kinetic energy of geostrophic velocity residuals per unit of mass, evaluated for each daily value of U'_G and defined as:

$$\mathrm{KE} = \frac{1}{2} U'^2_G + V'^2_G; \quad (6)$$

The Hovmoller diagrams of the KE in the period 1999–2009 were computed along the Anatolia and Crimean-Caucasian coasts.

Finally, the combined dataset was used to reconstruct the relative vorticity (ζ) field associated with the surface circulation in the region of Batumi Eddy (BE) and Sevastopol Eddy (SE). The relative vorticity was evaluated as the vertical component of the velocity field curl (Pedlosky, 1987):

$$\zeta = (\nabla \times v)_z = \frac{\partial v}{\partial x} - \frac{\partial u}{\partial y} \quad (7)$$

OSD
10, 1505–1524, 2013

M. Menna and P. -M. Poulain

3 Results and discussion

The unbiased pseudo-Eulerian velocity statistics (Fig. 1c) depict the well known characteristics of the mean circulation in the upper layer of the BS suggested by several authors in the past (e.g. Korotaev et al., 2001; Poulain et al., 2005), including the RC, BE and SE. However they add new information about the seasonal and interannual characteristics of the surface circulation in the BS.

3.1 Seasonal variability

Seasonal variations are emphasized by removing the mean velocity field (Fig. 1c) from the mean seasonal current fields; the resulting anomalies are shown in Fig. 2. Anomalies larger than 8-10 cm s^{-1} are observed in the BE (41–43° N; 39.5–42° E) and SE (43.5–45° N; 30.5–32.5° E) regions and east of the Crimean Peninsula. The cyclonic RC is stronger in winter (mean anomalies of about 4–5 cm s^{-1}; maximum values larger than 10 cm s^{-1} along the Anatolia and Crimea coasts and in the BE; Fig. 2a) and weaker in spring/fall (mean anomalies of about 2 cm s^{-1}; Fig. 2b and d) and summer (the anticyclonic anomalies of RC indicate that the summer currents are 4–5 cm s^{-1} smaller than the mean currents; Fig. 2c). The BE is characterised by an intense cyclonic circulation in winter, in agreement with Poulain et al. (2005), and an anticyclonic circulation in summer; the SE is most intense in spring.

3.2 Interannual variability

3.2.1 Mean flow

The MKE computed on a yearly basis is used to describe the annual variation of the mean circulation. The annual maps (Fig. 3) depict a more intense RC circuit in the period 2002–2006 with speeds of 20–40 cm s^{-1} and MKE larger than 250 $cm^2\,s^{-2}$; maximum values are observed along the Anatolia (600–700 $cm^2\,s^{-2}$) and Crimea (500 $cm^2\,s^{-2}$) coasts. Generally, the northwest branch of the Rim Current is weaker

OSD
10, 1505–1524, 2013

with speeds of 5–15 cm s^{-1} and values of MKE smaller than 150 $cm^2 s^{-2}$; larger intensities in this area are observed in 2002 and in the period 2005–2006 (speeds of 20–25 cm s^{-1} and MKE larger than 200 $cm^2 s^{-2}$). The RC surrounds two cyclonic structures (described in the previous studies as the Western and Eastern Gyres), that show the same characteristics over the whole study period (speeds smaller than 10 cm s^{-1} and MKE of 50–70 $cm^2 s^{-2}$).

The annual maps of EKE (Fig. 4) reach higher values in the Batumi region (larger than 250 $cm^2 s^{-2}$) in 2002, in the Sevastopol region (larger than 150 $cm^2 s^{-2}$) in 2000 and 2005, and in both these regions in 2003, 2004, 2006 and 2008; in 2003 high energy values are reached also along the western coast of the BS and along the Crimean coast.

3.2.2 Mesoscale eddies

The bin-size (0.25° × 0.25° × 1 day) was chosen as a compromise to resolve the basin and sub-basin (50–100 km) circulation of the BS and also to have a statistically significant number of drifter data inside each bin. Mesoscale (5–10 km) velocities are mostly included in the velocity variance and in the eddy kinetic energy. In particular, the KE can be used as a good indicator to follow the seasonal and interannual evolution of the mesoscale structures, as its large and variable values coincide with the main locations of the mesoscale eddies along the coasts of the BS (Fig. 5). The Hovmoller diagram in Fig. 5a, computed by meridionally averaging each KE value between 41° N and 42.5° N, illustrates the interannual changes in intensity and location of the mesoscale eddies off the Anatolia coast (28.5–39° E). The Bosphorus Eddy is a recurrent structure located near 28–29° E with values of KE generally smaller than 200 $cm^2 s^{-2}$; its energy increases without a specific periodicity (as in March 2001, July 2006, November–December 2007); sometimes it moves eastward and interacts with the close Sakarya Eddy (August–October 2003, October 2005, January 2006, December 2008–January 2009) reaching KE values larger than 500 $cm^2 s^{-2}$. The interaction

OSD
10, 1505–1524, 2013

M. Menna and P. -M. Poulain

between the Bosphorus and the Sakarya eddies confirms the description of Korotaev et al. (2003). The Sakarya Eddy, located around 31° E, prevails only in some years (2000, 2002, 2003, 2005, 2006, 2009) with KE values larger than 250 $cm^2 s^{-2}$. Figure 5a shows the presence of another eddy between 32–33° E with a quasi-persistent nature and KE signal between 150 $cm^2 s^{-2}$ and 250 $cm^2 s^{-2}$; this structure can moves westward and interact with the Sakarya Eddy (2005–2006). A mesoscale feature in this area was already recognised by Korotaev et al. (2003); according to its geographical location along the coast of the Province of Bartin we define this structure as the Bartin Eddy. The Sinop and Kizilirmak Eddies, located between 34.5° and 37°, show a quasi-permanent nature, in contrast with the results of Korotaev et al. (2003), and high values of KE (200–600 $cm^2 s^{-2}$) throughout the period considered; highest KE signal is observed in the period August–October 2003 in concomitance with the maximum intensities of the Bosphorus Eddy.

The diagram in Fig. 5b, computed by meridionally averaging each KE value between 43.5° N and 45° N, includes the Caucasus coast and the eastern side of the Crimean Peninsula (34–39.25° E). The Crimea Eddy is a quasi-permanent mesoscale feature, located between 34.5–35.5° E, characterised by a pronounced interannual variability in terms of KE and a zonal extension of the eddy. The KE signal shows generally higher values (larger than 500 $cm^2 s^{-2}$) when the Crimea Eddy becomes larger (1999, 2003, 2006, 2008). Another mesoscale eddy, identified by Korotaev et al. (2003) as the Kerch Eddy, is located between 36° E and 37° E (KE values of 250–400 $cm^2 s^{-2}$); it occurs sporadically and persists for a few months. The Caucasus Eddy, located around 37–38° E, is a sporadic structure with KE larger than 200 $cm^2 s^{-2}$, that occurs in the same periods as the Kerch Eddy and sometimes interacts with it (2003, 2004, 2006, 2007). The interactions among the Kerch Eddy, the Caucasus Eddy and the RC confirm the previous results of Korotaev et al. (2003) while their temporal intermittence contradicts these results. The Sukhumi Eddy (38.5–39.25° E) reveals a quasi-permanent nature with greater intensities during the winter and fall months (KE values of 200–400 $cm^2 s^{-2}$); it merges with the close Caucasus Eddy in winter 2003, fall 2007 and

OSD
10, 1505–1524, 2013

winter–spring 2008. The permanent nature of the Sukhumi Eddy contradicts the results of Korotaev et al. (2003).

3.2.3 Sub-basin scale eddies

The variability of the major sub-basin structures in the BS (the BE and the SE) is investigated using the spatially averaged time-series of KE (Figs. 6a and 7a) computed in the eddy regions. The BE is more intense in 2002–2006 and 2008 with typical values of KE between 200 $cm^2 s^{-2}$ and 300 $cm^2 s^{-2}$ (Fig. 6a); this structure is usually characterised by a diameter of ∼ 100 km and is located in the south-east corner of the BS. Periods of intense activity are observed during summer–fall 2002, fall 2004–winter 2005, summer 2006 and spring–fall 2008, when the BE shows greater KE (values larger than 400 $cm^2 s^{-2}$) and speeds larger than 30 $cm s^{-1}$ (Fig. 6c). The activity of BE is weaker in the period 1999–2001 and 2007 (Fig. 6a). Reversals of the surface circulation in the Batumi region are documented using the time-series of the spatially averaged ζ (Fig. 6b). The typical anticyclonic pathway, characterised by negative vorticity values, is sometimes interrupted by a cyclonic regime (positive vorticity). The main cyclonic circulation events are observed is spring–summer 2000, winter 2002 and 2003, fall 2004–early winter 2005, fall 2008–early winter 2009 (black arrows in Fig. 6b). High value of KE correspond to anticyclonic rotation. Examples of anticyclonic and cyclonic regimes are shown in Fig. 6c and d, respectively.

The SE is characterised by low energy levels with respect to the BE (Fig. 7a); maximum mean value of KE (∼ 300 $cm^2 s^{-2}$) is observed in fall 2000. During the period 2003–2007 the SE shows a pronounced seasonal variability, with higher KE in spring and fall and lower KE in winter and summer. The activity of SE is weaker in 2001–2002 and more intense in 2008. The time-series of the spatially averaged ζ (Fig. 7b) show that the SE is always anticyclonic, except for a cyclonic event in summer-fall 2008 probably due to the intrusion of an RC cyclonic meander in the Sevastopol region. The generation of SE is related to the meandering of the RC in the Sevastopol area and is generally observed in spring (speeds of about 15–20 $cm s^{-1}$; Fig. 7c).

OSD
10, 1505–1524, 2013

M. Menna and
P. -M. Poulain

4 Conclusions

The surface geostrophic circulation in the BS has been described combining 11 yr of drifter and satellite altimetry data in order to construct a regularly sampled dataset of observations less affected by the non-uniform drifter sampling. The mean geostrophic currents derived from the combined method (Fig. 1c) can be considered more realistic and accurate than the currents estimated from the SMDT of Kubryakov and Stanichny (2011) for different reasons: (1) the combined method is based on concurrent drifter and altimetry data for the period considered, whereas the synthetic method considers in-situ measurement and altimetry data collected in different time periods and the resulting SMDT is referred to the period in which the SLA data are referenced, whatever is the time measurement of the in-situ and altimetry data; (2) the SMDT is estimated without removing the wind-induced slips and the wind-driven Ekman currents from the drifter velocities, assuming that the wind–driven component (direct slip and Ekman component) is negligible. Actually, according to Poulain et al. (2012) the wind–driven component varies between the 0.5 % (for the SVP drogued drifters) and the 2 % (for the CMOD drifters) of the wind speed and represents a significant portion of the drifter velocity variance (1–27 %); therefore, it is not negligible and has to be removed in order to obtain the geostrophic velocities from drifter data.

The combined dataset: (1) gives more accurate descriptions of the mean flow seasonal variability, showing the RC stronger in winter, the BE stronger in winter/summer and the SE most intense in spring; (2) provides new descriptions of the mesoscale eddies, in particular the interaction between the Sinop and the Kizilirmak eddies located along the Anatolia coast and the interaction among the Kerch, the Caucasus and the Sukhumi eddies located along the Caucasus coast; (3) defines the persistence and the seasonal and interannual variations of the mesoscale and sub-basin eddies; (1) resolves a new quasi-persistent mesoscale eddy generated along the Anatolia coast and defined as the Bartin Eddy; (2) quantifies the inversions of surface circulation in the Batumi region.

OSD
10, 1505–1524, 2013

M. Menna and P. -M. Poulain

Acknowledgements. The authors would like to thanks all the people who deployed drifters in the Black Sea. The altimeter products were produced by SSALTO/DUACS and distributed by AVISO, with support from CNES (http://www.aviso.oceanobs.com/duacs/).

References

Atlas, R., Ardizzone, J. V., Hoffman, R., Jusem, J. C., and Leidner, S. M.: Cross-calibrated, multi-platform ocean surface wind velocity product (MEaSUREs Project), Guide Document, Physical Oceanography Distributed Active Archive Center (PO.DAAC), JPL, Pasadena, California, Version 1.0., 26 pp., 2009.

Centurioni, L. R., Ohlmann, J. C., and Niiler, P. P.: Permanent meanders in the California Current System, J. Phys. Oceanogr., 38, 1690–1710, doi:10.1175/2008JPO3746.1, 2008.

Centurioni, L. R., Niiler, P. N., and Lee, D.-K.: Near surface circulation in the South China Sea during the winter monsoon, Geophys. Res. Lett., 36, L06605, doi:10.1029/2008GL037076, 2009.

Korotaev, G., Oguz, T., Nikiforov, A., and Koblinsky, C.: Seasonal, interannual, and mesoscale variability of the Black Sea upper layer circulation derived from altimeter data, J. Geophys. Res., 108, 3122, doi:10.1029/2002JC001508, 2003.

Korotaev, G. K., Saenko, O. A., and Koblinsky, C. J.: Satellite altimetry observations of the Black Sea level, J. Geophys. Res., 106, 917–933, doi:10.1029/2000JC900120, 2001.

Kubryakov, A. A. and Stanichny, S. V.: Mean Dynamic Topography of the Black Sea, computed from altimetry, drifter measurements and hydrology data, Ocean Sci., 7, 745–753, doi:10.5194/os-7-745-2011, 2011.

Kundu, P. K.: Ekman veering observed near the ocean bottom, J. Phys. Oceanogr., 6, 238–242, 1976.

Menna, M., Poulain, P.-M., Zodiatis, G., and Gertman, I.: On the surface circulation of the Levantine sub-basin derived from Lagrangian drifter and satellite altimetry data, Deep-Sea Res., 65, 46–58, doi:10.1016/j.dsr.2012.02.008, 2012.

Niiler, P. P., Maximenko, N. A., Panteleev, G. G., Yamagata, T., and Olson, D. B.: Near-surface dynamical structure of the Kuroshio Extension, J. Geophys. Res.-Oceans, 108, 3193, doi:10.1029/2002JC001461, 2003.

Pedlosky, J.: Geophysical Fluid Dynamics, 2nd Edn., 710 pp., Springer, New York, 1987.

Poulain, P.-M., Barbanti, R., Cecco, R., Fayes, C., Mauri, E., Ursella, L., and Zanasca, P.: Mediterranean surface drifter database: 2 June 1986 to 11 November 1999, Rel. 75/2004/OGA/31, OGS, Trieste, Italy (CDRom), 2004.
Poulain, P.-M., Barbanti, R., Motyzhev, S., and Zatsepin, A.: Statistical description of the Black Sea near-surface circulation using drifter in 1999–2003, Deep-Sea Res. I, 52, 2250–2274, doi:10.1016/j.dsr.2005.08.007, 2005.
Poulain, P.-M., Gerin, R., Mauri, E., and Pennel, R.: Wind Effects on Drogued and Undrogued Drifters in the Eastern Mediterranean, J. Atmos. Ocean Technol. 26, 1144–1156, 2009.
Poulain, P.-M., Menna M., and Mauri, E.: Surface geostrophic circulation of the Mediterranean Sea derived from drifter and satellite altimeter data, J. Phys. Oceanogr., 42, 973–990, doi:10.1175/JPO-D-11-0159.1, 2012.
Rio, M.-H. and Hernandez, F.: A mean dynamic topography computed over the world ocean from altimetry, in-situ measurements, and a geoid model, J. Geophys. Res., 109, C12032, doi:10.1029/2003JC002226, 2004.
Rio, M.-H., Poulain, P.-M., Pascual, A., Mauri, E., Larnicol, G., and Santoleri, R.: A Mean Dynamic Topography of the Mediterranean Sea computed from altimetric data, in-situ measurements and a general circulation model, J. Mar. Syst., 65, 484–508, doi:10.1016/j.jmarsys.2005.02.006, 2007.
Uchida, H. and Imawakki, S.: Eulerian mean surface velocity field derived by combining drifter and satellite altimetry data, Geophys. Res. Lett., 30, 1229, doi:10.1029/2002GL016445, 2003.

OSD
10, 1505–1524, 2013

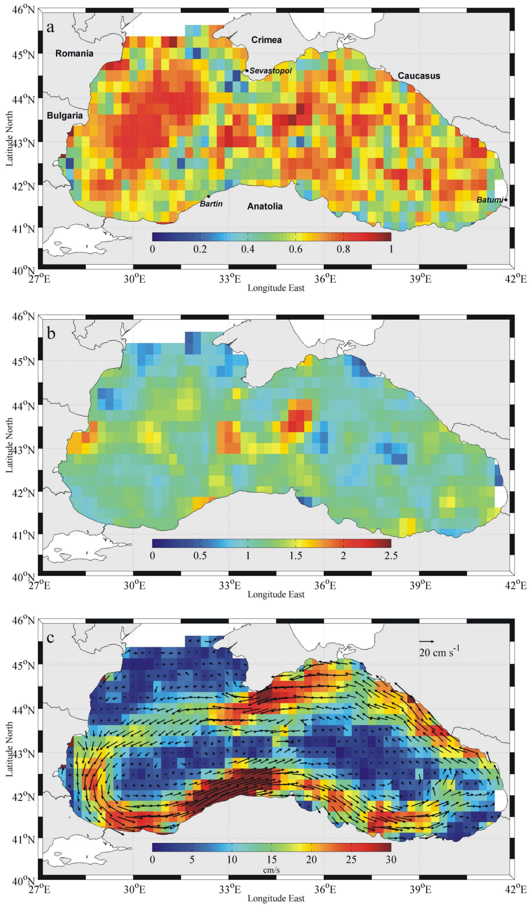

Fig. 1. Spatial distribution of the magnitude of: **(a)** the complex correlation between drifter geostrophic velocities U_{DG} and satellite anomalies of surface geostrophic velocities U_{SLA}; **(b)** the low pass filtered slope $|A|$ and **(c)** the offset B depicted with vectors and colors.

OSD
10, 1505–1524, 2013

M. Menna and P. -M. Poulain

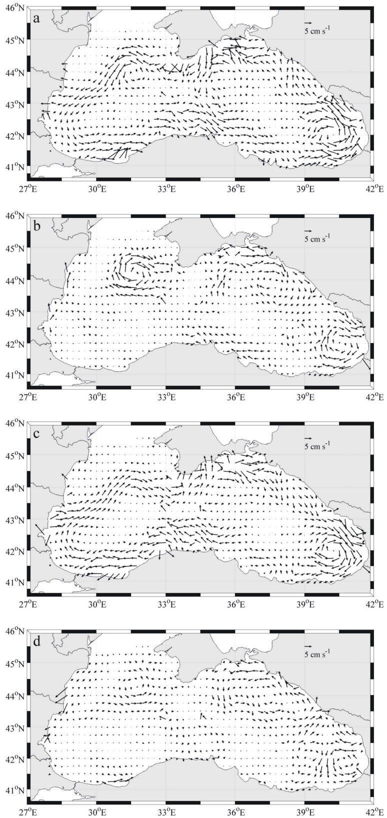

Fig. 2. Unbiased estimates of the anomalies of the mean surface geostrophic circulation in the Black Sea during **(a)** winter (January–March), **(b)** spring (April–June), **(c)** summer (July–September), **(d)** fall (October–December), in spatial bins of 0.25 × 0.25 and for the period 1999–2009.

OSD
10, 1505–1524, 2013

Geostrophic currents and kinetic energies in the Black Sea

M. Menna and P. -M. Poulain

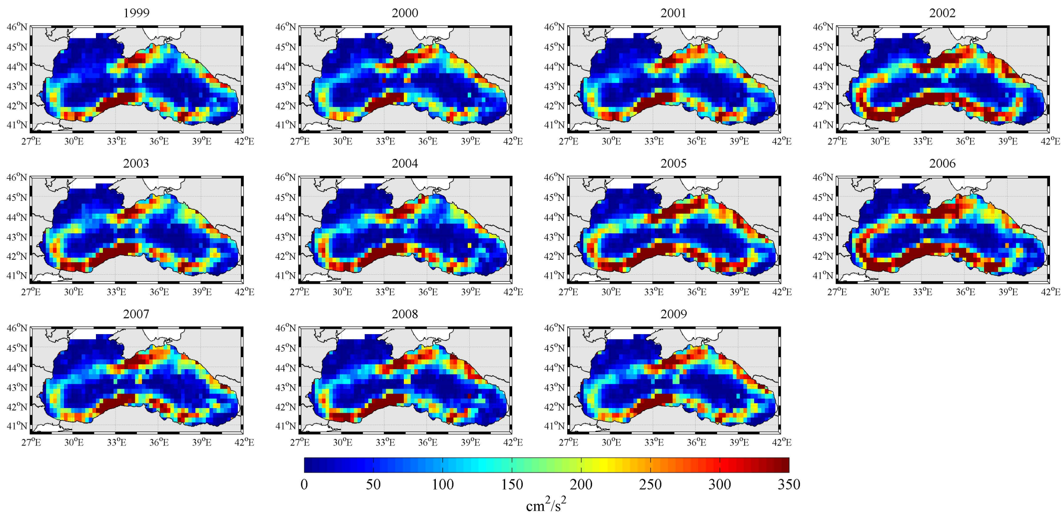

Fig. 3. Unbiased annual statistics of mean kinetic energy of the surface geostrophic currents in the period 1999–2009.

OSD

10, 1505–1524, 2013

M. Menna and P. -M. Poulain

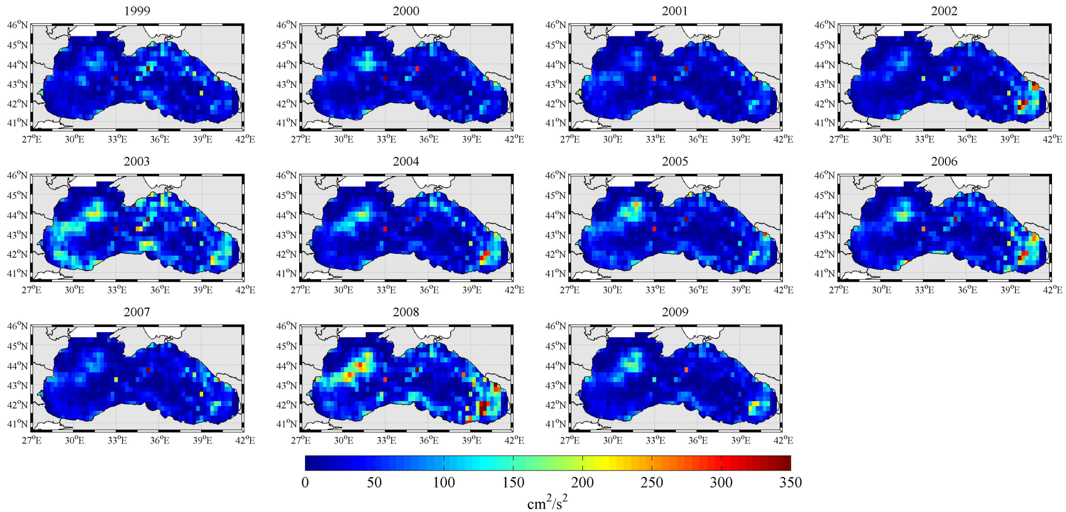

Fig. 4. Unbiased annual statistics of eddy kinetic energy of the surface geostrophic currents in the period 1999–2009.

OSD
10, 1505–1524, 2013

Geostrophic currents and kinetic energies in the Black Sea

M. Menna and P. -M. Poulain

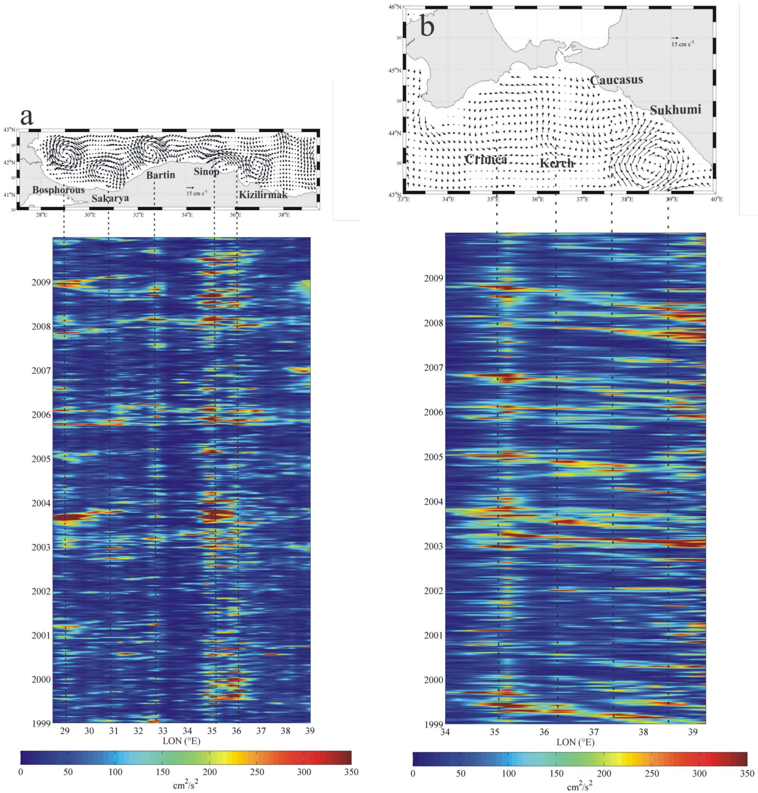

Fig. 5. Hovmoller diagrams of KE over **(a)** Anatolia and **(b)** Crimea-Caucasus coasts. In the upper panels daily snapshots of the anomalies of surface geostrophic velocities (3 May 2001 and 15 January 1999, respectively) indicate the location of the main eddies along the BS coasts; these anomalies are depicted with the original spatial resolution of AVISO products (1/8°) in order to better discriminate the mesoscale structures. Dashed lines mark the locations of mesoscale eddies.

OSD
10, 1505–1524, 2013

Geostrophic currents and kinetic energies in the Black Sea

M. Menna and
P. -M. Poulain

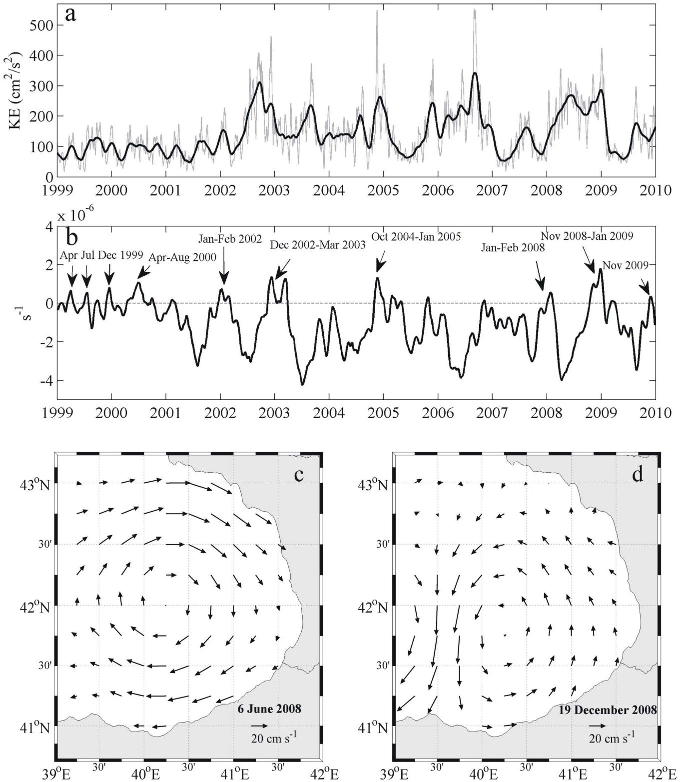

Fig. 6. (a) Time-series of KE spatially averaged in the region of BE (41–43° N; 39–42° E); grey line represent the daily time-series while the black line is the 90-day moving average of KE. **(b)** Time-series of the spatially averaged relative vorticity of the surface geostrophic currents in the region of BE; black arrows emphasize the main periods of cyclonic circulation. Snapshots of the **(c)** anticyclonic and **(d)** cyclonic circulation (U_G) over the Batumi area.

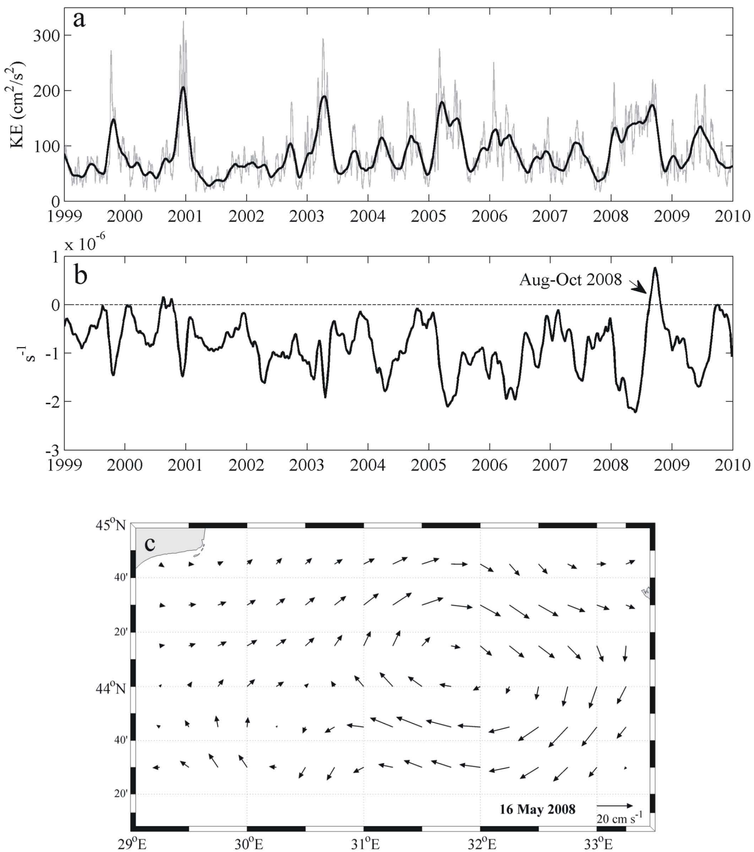

Fig. 7. (a) Time-series of KE spatially averaged in the region of SE (43.75–44.75° N; 30–33° E); grey line represent the daily time-series while the black line is the 90-day moving average of KE. **(b)** Time-series of the spatially averaged relative vorticity of the surface geostrophic currents in the region of SE; black arrow indicate the period characterised by cyclonic circulation. **(c)** Snapshot of geostrophic currents (U_G) in the region of SE.

OSD
10, 1505–1524, 2013

Geostrophic currents and kinetic energies in the Black Sea

M. Menna and
P. -M. Poulain